35th Annual International Conference of the IEEE EMBS
Osaka, Japan, 3 - 7 July, 2013

Impact of bipolar electrodes contact on fractionation index measurement

Nicolas Navoret, Sabir Jacquir, Gabriel Laurent, Stéphane Binczak

Abstract— **Signals such as Complex Fractionated Atrial Electrograms (CFAE) are tracked during ablation procedures to locate the arrhythmical substrate regions. Most of CFAE classification tools use fractionation indexes. However, recordings from intracardiac catheter depend on electrode contact quality. This paper investigates the impact of electrode contact area on fractionation indexes. It is assessed through three kinds of arrhythmical activations resulting from a numerical simulation of a small piece of the cardiac tissue. Bipolar electrograms are extracted corresponding to 25 different contact areas and fractionation indexes (Shannon entropy, non linear energy operator and maximum peak ratio) are computed. Results yield that the Shannon entropy offers a good potential discrimination between arrhythmic scenarios and is less sensitive to the electrode contact variation.**

I. INTRODUCTION

During Atrial Fibrillation (AF), atria are contracted and activated rapidly and irregularly. Some underlying mechanisms of AF were identified such as reentrant activity or ectopic foci [1]. Among existing AF treatments, radiofrequency ablation appears to be one of the most efficient. It consists in an ablation of the arrhythmical substrate regions using an intracardiac catheter. Before ablation, the practitioner explores atria cavities using the catheter as a bipolar electrode to find electrical signals, symptomatic of abnormal activity. Some signals have been presented in literature as particularly involved in AF maintenance, these are Complex Fractionated Atrial Electrograms (CFAE) [2]. CFAE are now used in ablation procedures to guide the electrophysiologist through atrial regions to ablate or isolate AF sources; this process is known as electrogram guided therapy [3-5]. Unfortunately there is no consensus yet about the way to handle these electrograms (EGM) and several definitions can be found in literature for CFAE signals. To date, electrophysiologists are still using visual recognition to detect CFAE. Several studies have proposed classifications for CFAE in order to cluster the huge variety of intraatrial signals that falls into the definition boundaries. Classification mostly relies on signal fractionation measurement. Some indexes are given, based on signal processing tools to quantify fractionation from CFAE activation patterns [6-8]. Fractionated electrograms are extracellular potentials presenting multiple deflections that result from local asynchronous activation of atrial substrate beneath the recording electrodes. Reliable measurements require a stable and constant acquisition process, however the catheter disposal is different for each new spot. The applied pressure, the angle, the contact surface between the metal electrode and the substrate are changing every time, with every heart beat. Several studies in medical domains investigate the impact of contact quality on electrogram acquisition and reveal this is a major parameter to take into account [9-11]. This work presents bipolar electrogram recordings made on a simulated substrate. The Aliev Panfilov model is applied to a 2D surface to simulate a piece of cardiac tissue. Disturbances are created to obtain typical AF activation scenarios. Electrograms are acquired using a numerical model of the ablation catheter tip. Bipolar EGM are collected for several electrode contact surfaces. Three indexes are then applied to quantify fractionation on the resulting electrograms, the Shannon entropy, the Nonlinear Energie Operator (NLEO) and the Maximum Peak Ratio (MPR). Impact of electrode contact area on these indexes values will be discussed.

N. Navoret, S. Jacquir, and S. Binczak are with the Laboratoire LE2I UMR CNRS 6306, Université de Bourgogne, 9 avenue Alain Savary, BP47870, 21078 Dijon, France sabir.jacquir@u-bourgogne.fr

II. MATERIALS

A. Aliev Panfilov Model

This behavioral model is a modification of the Fitzhugh Nagumo model of an excitable medium. It reproduces most of the basic properties of cardiac cells such as depolarization and repolarization phases of the action potential [12]. The simplicity of this model makes it possible to simulate large surface of cardiac tissue without using large computing resources. Two differential equations describe the fast and slow processes, presented here for monodomain in a 2D isotropic implementation:

$$\begin{cases} \dfrac{\partial e}{\partial t} = \delta \nabla^2 e - k(e-a)(e-1) - er + I_{stim}, \\ \dfrac{\partial r}{\partial t} = [\varepsilon + \dfrac{\mu_1 r}{\mu_2 + e}][-r - ke(e-b-1)] \end{cases} \quad (1)$$

where e is the membrane potential, r is the conductance of the inward currents, these variables are dimensionless here. k, a, b, μ_1, μ_2 are parameters determined from experiments. With δ the diffusion parameter and ∇^2 the Laplacian operator. I_{stim} is the potential used to initiate the first excitation. Default values given in the Panfilov model description are: $\varepsilon = 0.002$; $a = b = 0.15$; $\mu_1 = 0.2$; $\mu_2 = 0.3$; $k = 8$; $\delta = 0.05$ This model allows spiral waves and break up to be initiated easily. This model is suitable to investigate qualitatively some scenarios occurring during AF. For a comparison with a realistic case, it will be necessary to use an ionic model of atrial cell (for example Courtemanche-Ramirez-Nattel model [13]).

978-1-4577-0216-7/13/$26.00 ©2013 IEEE

B. Catheter representation

The modeled catheter is a Thermocool irrigated tip ablation catheter from Biosense Webster (Biosense Webster, Diamond Bar, CA, USA). It is used by our colleague cardiologist to burn areas of atrial substrate responsible for AF maintenance or triggering during ablation therapy. The tip of the catheter is composed with four metallic electrodes used to acquire the atrial substrate fields of potentials. Most of the time, electrodes are used in pairs to acquire bipolar electrograms. Fig. 1.a) shows the Thermocool catheter tip, electrodes size and distribution. Only the distal pair of electrodes is modeled here. Recordings are made disposing the tip according to Fig. 1.b) configuration. For this study, only electrograms from the East-Center position are presented. The electrodes surfaces are 32.1 mm^2 for the distal one, 13.9 mm^2 for the 3 others. One chooses to keep one third of these values as average contact surface with the substrate. Chosen contact surface are thus 10.7 mm^2 for the distal electrode, 4.63 mm^2 for the 3 others. Taking into account average dimensions for a cardiomyocyte of 15 μm by 100 μm, about 7100 cells are covered by the distal electrode, the 3 others cover about 3000 cells each. These amounts are taking into account in further numerical simulations. Inspired from [14], the first temporal derivative of the transmembrane potential was calculated to retrieve extracellular potential. It gives an unipolar recording. The bipolar recording is the difference between two unipolar electrograms [15] from two different spatial positions. This measure yields a first spatial derivative. The potential recorded by an electrode is defined as the sum of potentials from cells covered by its contact surface. In the following simulations, areas of the electrodes

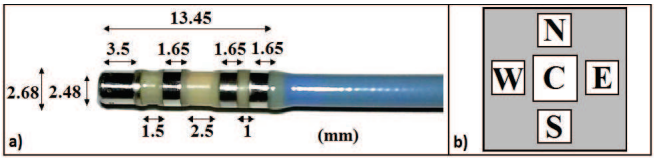

Fig. 1. a) Thermocool catheter tip, electrode size and distribution. b) Electrode disposal in the numerical substrate, representing 4 cardinal positions for catheter acquisition. C for Center electrode represents the distal one.

are modified to observe the impact on fractionation indexes. The electrode contact surface is expressed as the ratio of the full electrode area; for instance the 1/3 ratio means that only one third of the surface touches the substrate and will be indicated by a 3 in results ahead. This approach aims to reproduce the conditions of acquisition of an intracardiac electrogram during AF radiofrequency ablation. The quality of the contact between the catheter and the substrate is not constant and plays a significant role in the appearance of signals and therefore on quantification tools.

C. Fractionation analysis tools

Three indexes are proposed to discriminate the 3 scenarios of activation using different electrode contact ratios.

-**The Shannon Entropy** [16], it quantifies the statistical spread of the signal states at a given time.

-**The Non-Linear Energy Operator (NLEO)** [17, 18]. This index quantifies the energy requiered by a system to generate oscillations in a signal.

-**The Maximum Peak Ratio**: Two peak detections are applied to the signal; conditions for positive peak detection are:

$$P_j \equiv Mn_i + \Delta \leq Mx_j \bigcap Mn_{i+1} + \Delta \leq Mx_j \qquad (2)$$

With P for peak, Δ is the fixed threshold, Mn is the local minima and Mx is the local maxima. i and j indices refering to arbitrary samples in the signal. After a first peak detection whith no threshold, a kmeans clusterisation is applied on detected peaks. The second peak detection is applied using the maximum centroid value as a threshold. The MPR is the ratio between the number of maximum peaks from the first and the second peak detection.

III. Results

This section presents the 3 types of activation, with the respective electrograms acquired from the catheter tip model. The planar waves are induced by applying a stimulation

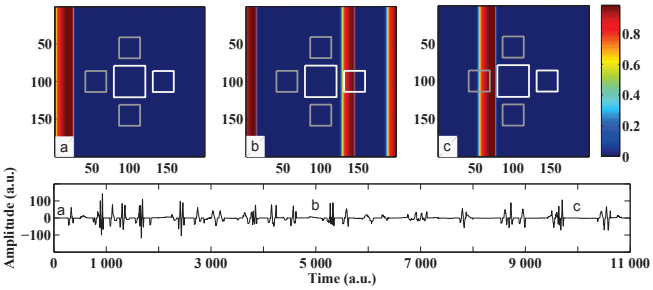

Fig. 2. Slightly arrhythmic planar waves and the corresponding bipolar electrogram for electrodes positioned on the East-Center configuration. The surface ratio is 1/3 for both electrodes. Activation maps are presented for times 100, 5000 and 10000 (a.u.).

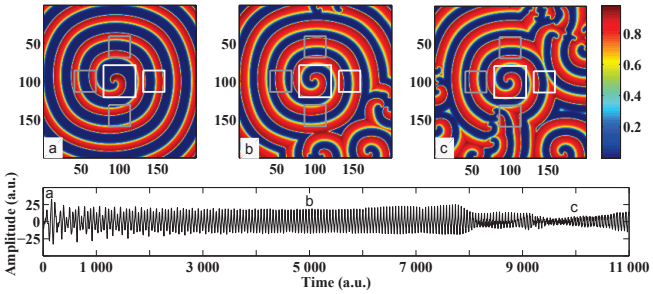

Fig. 3. Unstable spiral waves and the corresponding bipolar electrogram for electrodes positioned on the East-Center configuration. The surface ratio is 1/3 for both electrodes. Activation maps are presented for times 100, 5000 and 10000 (a.u.).

potential at different frequencies on the left edge of the matrix (Fig.2). The aim is to reproduce a planar propagation with variable frequencies mimicking a slightly arrhythmic situation. The spiral waves configuration (Fig.3) uses the same method but the planar front is set to zero when it reaches the half width of the matrix. This break causes the

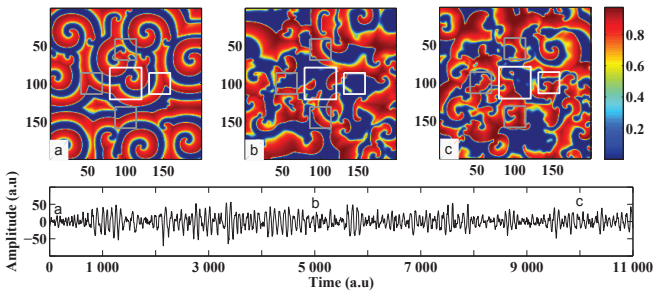

Fig. 4. Breaking waves and the corresponding bipolar electrogram for electrodes positioned on the East-Center configuration. The surface ratio is 1/3 for both electrodes. Activation maps are presented for times 100, 5000 and 10000 (a.u.).

wave to roll on it self and form a spiral. The instability is due to the used model parameters ($\varepsilon = 0.005$; $a = b = 0.095$; $\mu_1 = 0.15$; $\mu_2 = 0.3$; $k = 8$). The breaking waves scenario (Fig.4) is set up by applying a multiple spiral waves pattern to the matrix and using parameters leading to instability ($\varepsilon = 0.005$; $a = 0.08$; $b = 0.1$; $\mu_1 = 0.15$; $\mu_2 = 0.3$; $k = 8$). The Fig.2 shows irregular patterns with fractionation. This EGM has some fractionation similarities with CFAE, the activation pattern amplitude is greater than the 2 other EGM. The Fig.3 shows a large period of regular electrogram, this is due to a quasi synchronization between the activation acquired by both Central and East electrodes. The signal amplitude is the lowest for this signal suggesting that the bipolar acquisition induces a potential cancelation. Fig.4 shows very anarchic activation maps and the resulting EGM acts as well. This signal alternates periods of quasi sinusoid with periods of fractionation. The signal amplitude is approximately between the first 2 EGM. For each electrode the total metallic surface is successively divided by 2, 3, 5 , 8 and 10. The recorded activity will differ according to the substrate covered areas. Twenty five bipolar electrograms are then recorded using the 25 different electrodes area ratio combinations. Signals last 11000 points and are analyzed with a 1000 points step window, it yields 11 values for each ratio and index. For each of the 3 activation scenarios, the NLEO, entropy and MPR indexes are calculated. Fig.5 shows that planar waves

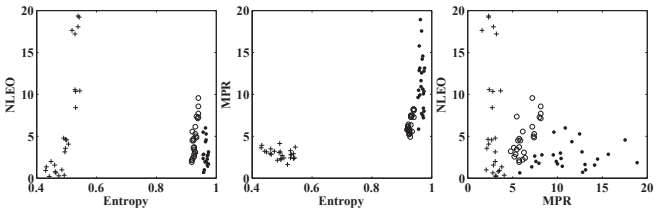

Fig. 5. Indexes mean values for the 3 activation scenarios and the 25 electrodes area ratios. (+) planar, (o) breaking, (.) spiral

are easily discriminated. The separation is less obvious for spiral and breaking configurations. Entropy seems to better discriminates these two kinds than the other indexes. It also appears than NLEO and MPR are more sensitive to the electrode area than entropy. Figs. 6, 7, 8 present the index

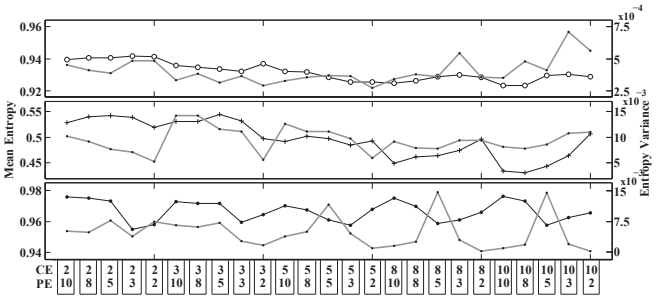

Fig. 6. (o) breaking, (+) planar, (.) spiral. The Entropy index mean value for each surface electrode ratio. Thin black line for mean and thick grey line for variance.

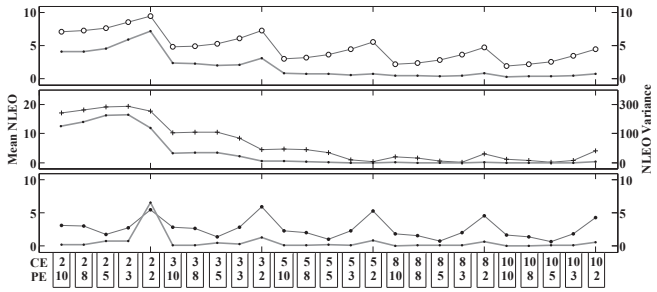

Fig. 7. (o) breaking, (+) planar, (.) spiral. The NLEO index mean value for each surface electrode ratio. Thin black line for mean and thick grey line for variance.

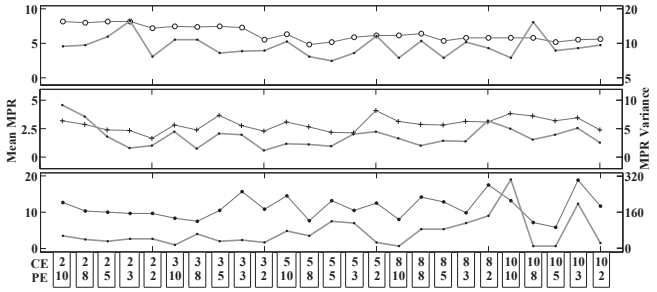

Fig. 8. (o) breaking, (+) planar, (.) spiral. The MPR index mean value for each surface electrode ratio. Thin black line for mean and thick grey line for variance.

mean value and variance for each electrode area ratio for each scenario. CE is for Central Electrode ratio, PE for Peripheral Electrode. For every ratio, the mean entropy index for breaking waves is almost constant (see Fig. 6). The planar waves entropy is lower than breaking and spiral values and displays changing variance. The mean entropy for spiral waves is above previous cases but shows irregular variance according to the ratio.

In Fig. 7 NLEO shows a large variability according to the ratios. Breaking waves NLEO shows a decreasing sawtooth behavior. Values decrease with the central electrode area reduction and increase with the peripheral electrode area

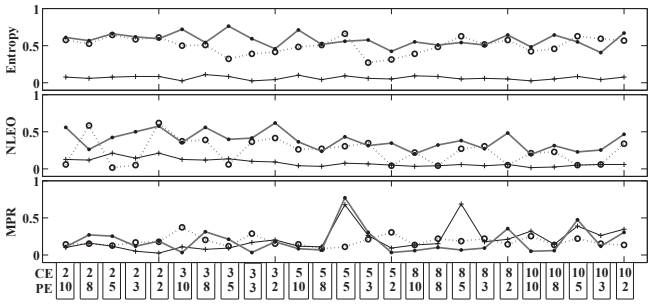

Fig. 9. Normalized euclidian distances between clustered data centers for the 3 indexes, Entropy, NLEO, MRP. (o) Distance breaking-planar, (+) distance breaking-spiral, (.) distance planar-spiral.

increases. The CE surface is bigger than the PE, changes of its contact area have a major impact on NLEO index. Planar waves values for NLEO are decreasing rapidly with the CE ratio and stabilize for weakest CE values, the variance tends to be quasi constant to. In the spiral scenario, NLEO varies slightly depending on the electrodes ratio. The NLEO variance has low values except for the 2/2 ratio, this could be explained by a desynchronization in the activity acquired by both CE and PE. Discrimination between scenarios might be possible for a given ratio but using this index for discrimination without a stable acquisition process is unreliable.
MPR index (see Fig.8) appears quite constant for breaking configuration, it slightly decreases with the central electrode contact reduction. The variance is much less stable. For the planar waves scenario, MPR values are lower here than for the breaking case. MPR values for spiral are higher than for the 2 previous cases. Mean value and variance are quite constant for the seven first ratios and then increases for the following ratios. This traduces the consequence of the CE contact area. In Fig. 9, indexes discrimination potential is assessed according to the 25 electrodes ratios. The three scenarios represent 3 classes whom indexes data were clustered using kmeans algorithm. A centroid is determined for each cluster. For a given electrode surface ratio, the euclidian distance between the 3 data classes is calculated and reported on the Fig. 9. The distance corresponding to the entropy and the NLEO measured between breaking and spiral scenarios are quasi-constant. That means that the electrode ratios do not influence the waveform. Entropy and NLEO distances display a better discrimination potential for the planar case to the spiral or to the breaking case. Using the maximum peak ratio, it is not possible to distinguish the three scenarios.

IV. Discussion & Conclusion

In this study, three typical arrhythmic substrate scenarios are simulated. Bipolar electrograms are recorded from the numerical substrate mimicking a catheter acquisition using 25 different electrode contact areas. EGM are submitted to 3 analysis tools to quantify the imbedded fractionation as usually done in CFAE classification process. The impact of electrode contact area differs from one index to another. It appears that the Shannon's entropy is more robust and still offer a good discrimination between scenarios. To validate the method used in this work, the simulation results will be compared with experimental and clinical data. It could be useful in the case of a classification tool implementation process or in the context of clinical data analysis where data acquisitions are subject to changing conditions. This completes the assessment of discriminative power for fractionation indexes.

References

[1] S. Nattel. Atrial electrophysiological remodeling caused by rapid atrial activation: underlying mechanisms and clinical relevance to atrial fibrillation. *Cardiovascular research*, 42(2):298–308, 1999.

[2] K. Nademanee, J. McKenzie, E. Kosar, and et al. A new approach for catheter ablation of atrial fibrillation: mapping of the electrophysiologic substrate. *Journal of the American College of Cardiology*, 43(11):2044–2053, 2004.

[3] H.L. Estner, G. Hessling, G. Ndrepepa, and et al. Electrogram-guided substrate ablation with or without pulmonary vein isolation in patients with persistent atrial fibrillation. *Europace*, 10(11):1281, 2008.

[4] M.W. Krueger, C. Schilling, and A. Luikand. Descriptors for a classification of complex fractionated atrial electrograms as a guidance for catheter ablation of atrial fibrillation. *Biomed Tech 2010*, 55 (Suppl. 1), 2010.

[5] M. Haïssaguerre, M. Hocini, P. Sanders, and et al. Catheter ablation of long-lasting persistent atrial fibrillation: Clinical outcome and mechanisms of subsequent arrhythmias. *Journal of cardiovascular electrophysiology*, 16(11):1138–1147, 2005.

[6] R.J. Hunter, I. Diab, M. Tayebjee, and et al. Characterization of fractionated atrial electrograms critical for maintenance of atrial fibrillationclinical perspective a randomized, controlled trial of ablation strategies (the cfae af trial). *Circulation: Arrhythmia and Electrophysiology*, 4(5):622–629, 2011.

[7] J. NG, A.I. Borodyanskiy, E.T. Chang, and et al. Measuring the complexity of atrial fibrillation electrograms. *Journal of Cardiovascular Electrophysiology*, 21(6):649–655, 2010.

[8] N. Navoret, S. Jacquir, G. Laurent, and et al. Recurrence quantification analysis as a tool for complex fractionated atrial electrogram discrimination. In *Annual International Conference of the IEEE EMBS*, pages 4185–4188. IEEE, 2012.

[9] D.D. Correa de Sa, N. Thompson, J. Stinnett-Donnelly, and et al. Electrogram fractionation the relationship between spatiotemporal variation of tissue excitation and electrode spatial resolution. *Circulation. Arrhythmia and electrophysiology*, 4(6):909–916, 2011.

[10] J.M. Stinnett-Donnelly, N. Thompson, N. Habel, and et al. Effects of electrode size and spacing on the resolution of intracardiac electrograms. *Coronary Artery Disease*, 23(2):126, 2012.

[11] N. Navoret, S. Jacquir, G. Laurent, and et al. Relationship between complex fractionated atrial electrogram patterns and different heart substrate configurations.

[12] R.R. Aliev and A.V. Panfilov. A simple two-variable model of cardiac excitation. *Chaos, Solitons & Fractals*, 7(3):293–301, 1996.

[13] M. Courtemanche, R.J Ramirez, and S. Nattel. Ionic mechanisms underlying human atrial action potential properties: insights from a mathematical model. *American Journal of Physiology-Heart and Circulatory Physiology*, 275(1):H301–H321, 1998.

[14] G.T.A. Kovacs. Electronic sensors with living cellular components. *Proceedings of the IEEE*, 91(6):915–929, 2003.

[15] F.J. Chorro, J. Guerrero, F. Pelechano, and et al. Influence of recording mode (unipolar or bipolar) on the spectral characteristics of epicardial recordings in ventricular fibrillation. an experimental study. *Revista española de cardiología*, 60(10):1059, 2007.

[16] C.E. Shannon. A mathematical theory of communication. *ACM SIGMOBILE Mobile Computing and Communications Review*, 5(1):3–55, 2001.

[17] J.F. Kaiser. On a simple algorithm to calculate the energy of a signal. In *Acoustics, Speech, and Signal Processing, 1990. ICASSP-90., 1990 International Conference on*, pages 381–384. IEEE, 1990.

[18] M.P. Nguyen, C. Schilling, and O. Dossel. A new approach for frequency analysis of complex fractionated atrial electrograms. In *Annual International Conference of the IEEE EMBS*, pages 368–371. IEEE, 2009.